Time-Domain Measurement of Ultrafast Magnetization Dynamics in Magnetic Nanoparticles

Masters of Science Thesis

Brian Egenriether

November 2015

UNIVERSITY OF SOUTH CAROLINA

Agenda

- Introduction and purpose
- Experimental objectives
- Theoretical introductions
- Inductive technique description
- Experimental details and considerations
- Results and interpretations
- Questions

UNIVERSITY OF SOUTH CAROLINA

Introduction and Purpose

- Magnetic nanoparticles composed of magnetite (Fe_3O_4) with a diameter of 10nm are studied.
- Similar particles are used in *in vivo* medical imaging, magnetic sensors, drug delivery, cancer research, and microscopic diffraction gratings (Crawford Group), etc.
- In practically all of these applications, the particles interact with fluctuating magnetic fields.
- Large amounts of frequency-domain research has been done on magnetic nanoparticles, however almost no time-domain data exists due to the smallness of the particles and the high speed of the process (~2ns).
- Having an idea of how they behave in the time domain yields a better understanding of how to employ them in practice.
- It also serves the field of scientific inquiry.

UNIVERSITY OF SOUTH CAROLINA

Experimental Objectives

- To determine if collections of magnetic nanoparticles undergo the precession dynamics predicted by the Landau-Lifshitz (LL) theory and if these time-domain dynamics can be measured by a magnetic induction technique to be described.
- To fit the time-domain data to a damped sinusoidal solution to the LL equation.
- To calculate the frequency-domain response by employing a Fast Fourier Transform to the time-domain data.
- To understand the progression of the frequency as a function of the applied magnetic bias field.
- To estimate the phenomenological damping parameter of the magnetite particles as a function of applied field and the spectroscopic splitting factor (or *g-factor*), of the particles.

UNIVERSITY OF SOUTH CAROLINA

Larmor Equation

$$\frac{d\overrightarrow{\boldsymbol{M}}}{dt} = \gamma\overrightarrow{\boldsymbol{M}} \times \overrightarrow{\boldsymbol{B}} = \gamma\mu_0\overrightarrow{\boldsymbol{M}} \times \overrightarrow{\boldsymbol{H}}$$

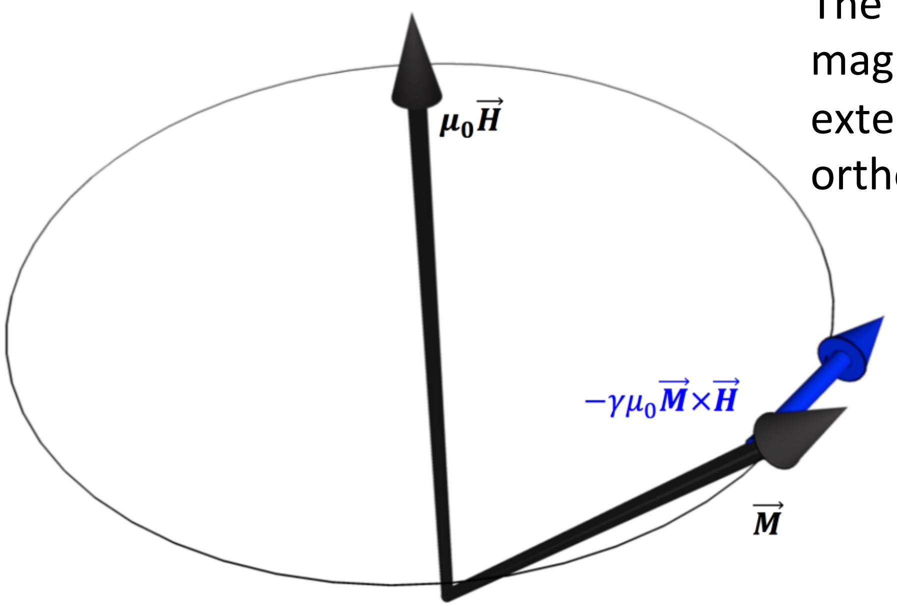

The Larmor equation predicts magnetization will precess about an external field indefinitely in a plane orthogonal to the field.

UNIVERSITY OF SOUTH CAROLINA

Landau-Lifshitz Theory

$$\frac{d\vec{\boldsymbol{m}}}{dt} = -\frac{\gamma}{1+\alpha^2}\mu_0\vec{\boldsymbol{m}} \times [\vec{\boldsymbol{H}} + \alpha(\vec{\boldsymbol{m}} \times \vec{\boldsymbol{H}})]$$

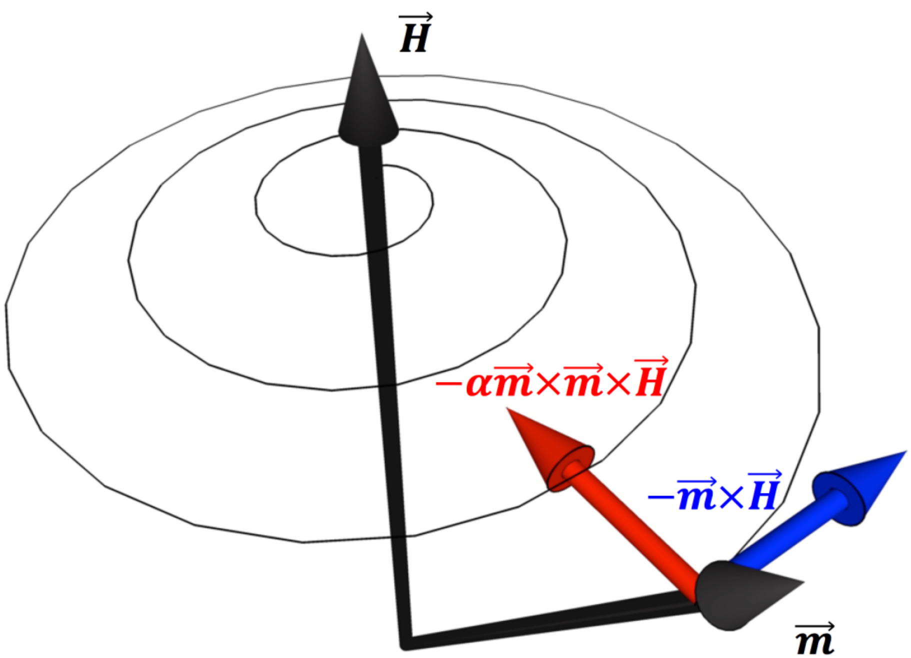

Due to losses with the surrounding medium, the magnetization vector follows the path of a decaying spiral as it undergoes dynamic precession. (Larmor + damping)

UNIVERSITY OF SOUTH CAROLINA

Inductive Technique Overview

Coplanar waveguide
With nanoparticle
sample

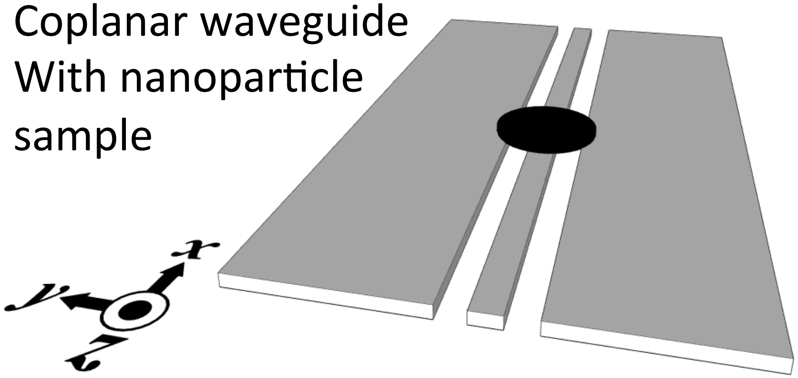

Rapid *H* field
reorientation

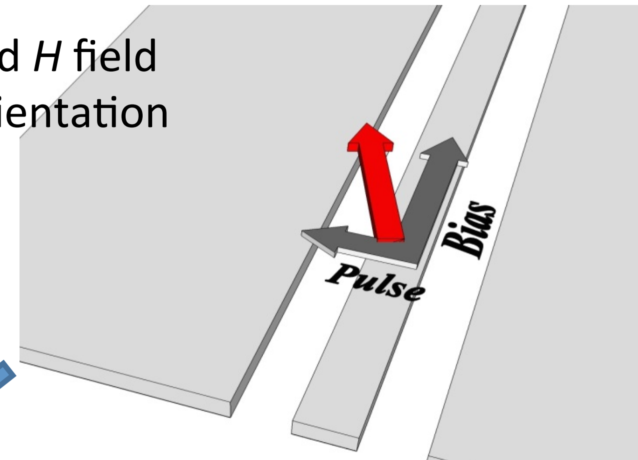

Time-changing
magnetic field
from particles

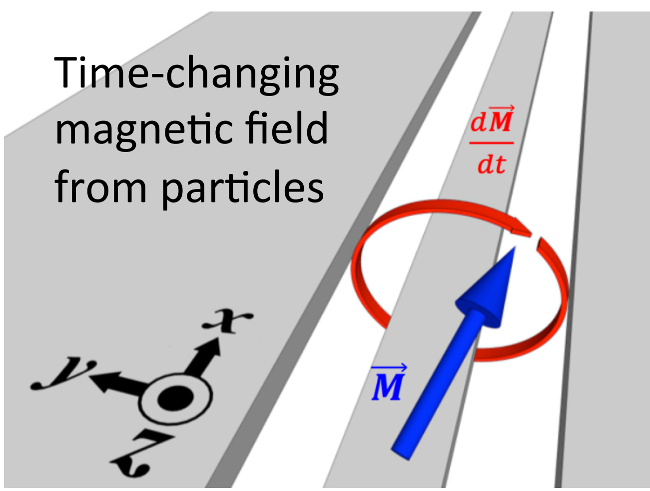

Induced voltage by
Faraday's Law

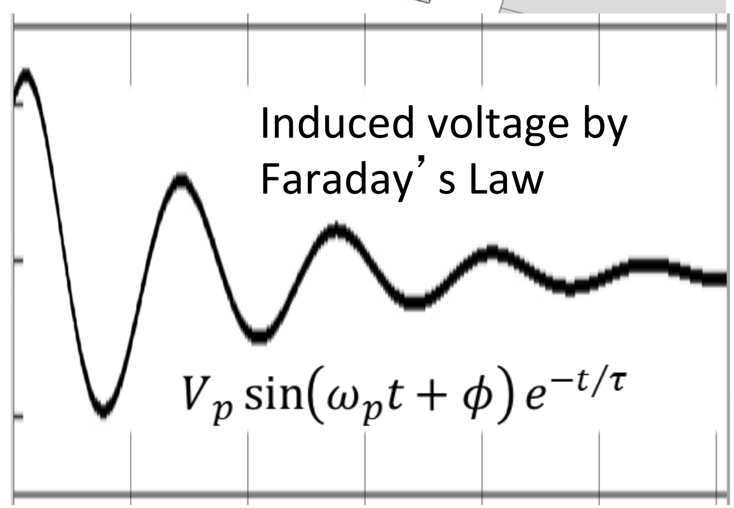

UNIVERSITY OF
SOUTH CAROLINA

Superparamagnetism

- Small magnetic particles have moments that fluctuate their orientation due to thermal excitations.
- For single particles above a certain temperature (the "blocking" temperature) the net magnetization over an extended time is zero.

$$\tau = \tau_0 e^{KV/k_B T}$$

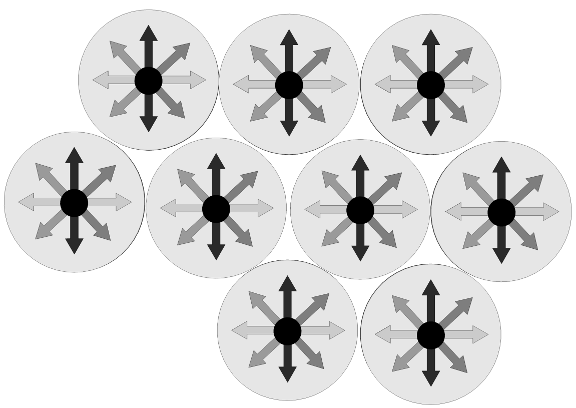

- The magnetization is a nonlinear function of the external magnetic field.
- This effect causes the M-H curve of the particles to close, exhibiting no remanence or coercivity.

- For dense collections of interacting particles however, the effective blocking temperature can be raised, inducing a *mixed-state* of ferrimagnetism and superparamagnetism.

UNIVERSITY OF SOUTH CAROLINA

Superparamagnetism

- In dense collections of interacting particles, the curve may not completely close nor cross identically at zero.
- The maximum value of magnetization M_s is found to be 532kA/m, which is roughly 10% higher than the tabulated value. Error in Fe_3O_4 concentration or volumetric measurements of ferrofluid could be the cause.
- Particles have also been found to have a higher M_s due to surface effects, but the converse has also been found.

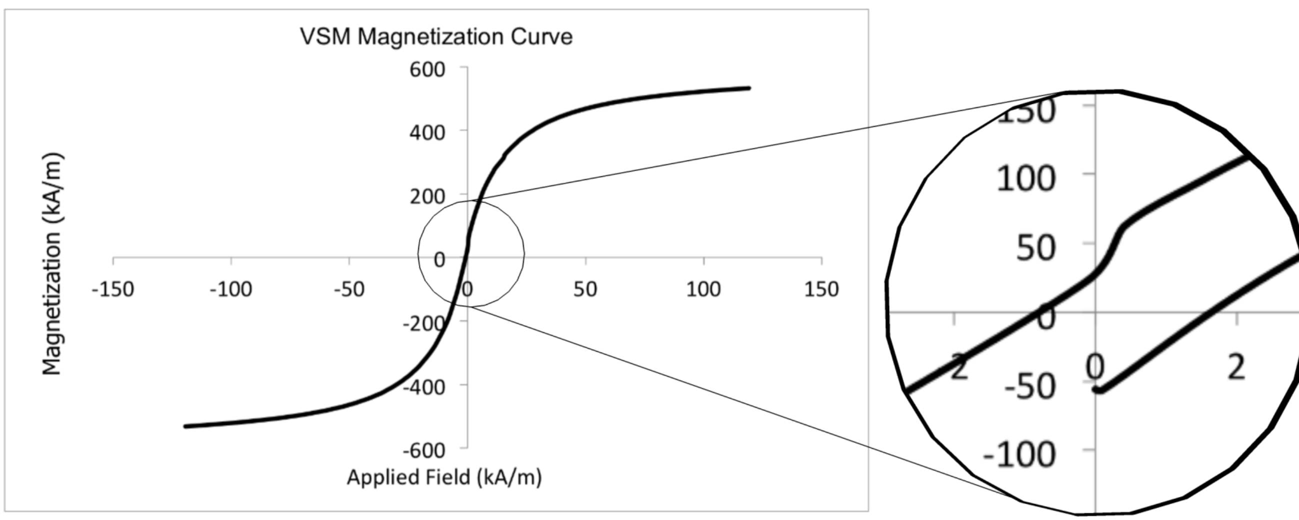

UNIVERSITY OF SOUTH CAROLINA

Two Sample Geometries

- Two types of nanoparticle sample geometries were prepared.
- Of these, half were dried in a directed magnetic field (2.5kA/m) and half were not.

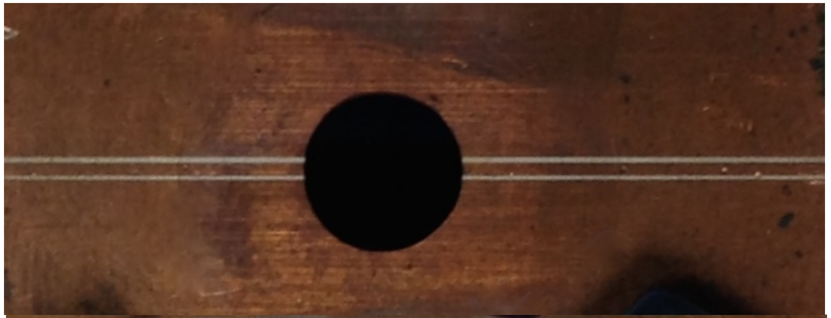

Circular sample on waveguide.

Strip sample on waveguide.

UNIVERSITY OF SOUTH CAROLINA

Experiment Layout

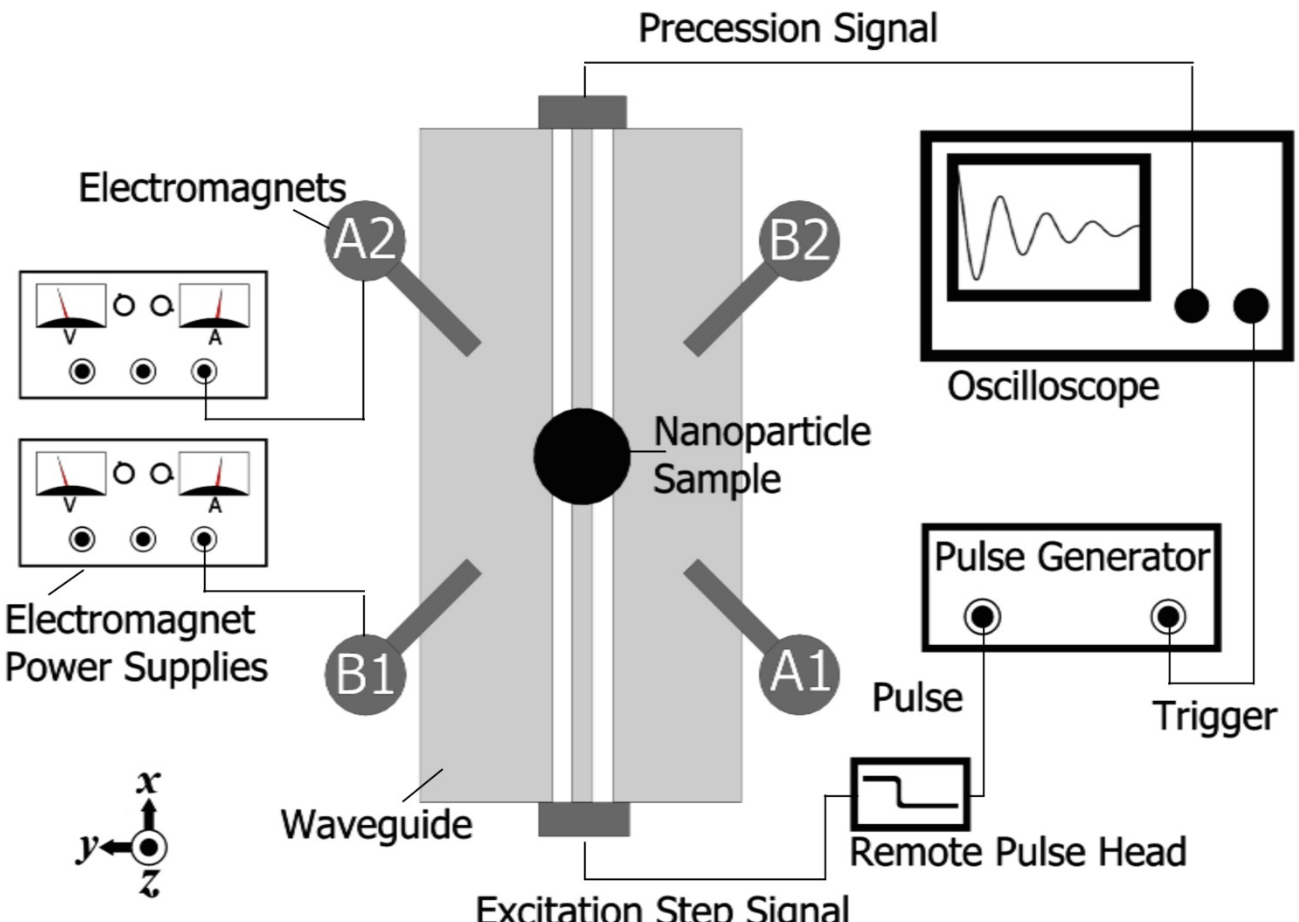

UNIVERSITY OF SOUTH CAROLINA

Temporal Drift Error Correction

To extract the inductive signal from the step voltage waveform subtractive synthesis is employed. A step signal without precession is subtracted from one that has precession, leaving only the desired inductive signal.

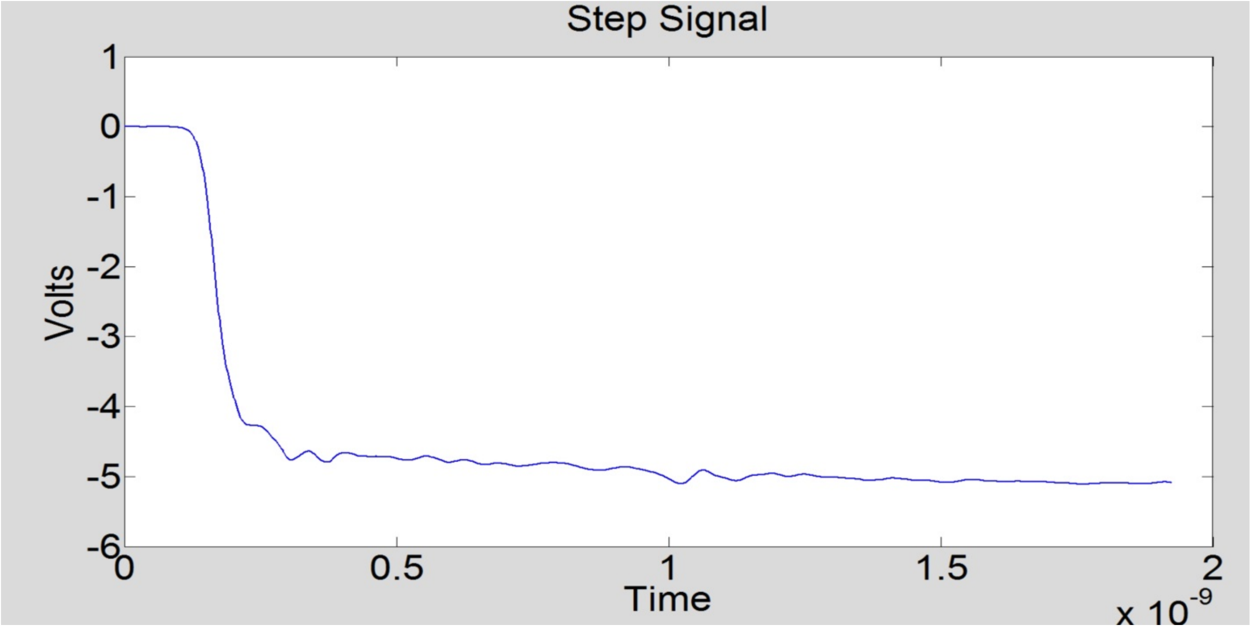

UNIVERSITY OF SOUTH CAROLINA

Temporal Drift Error Correction

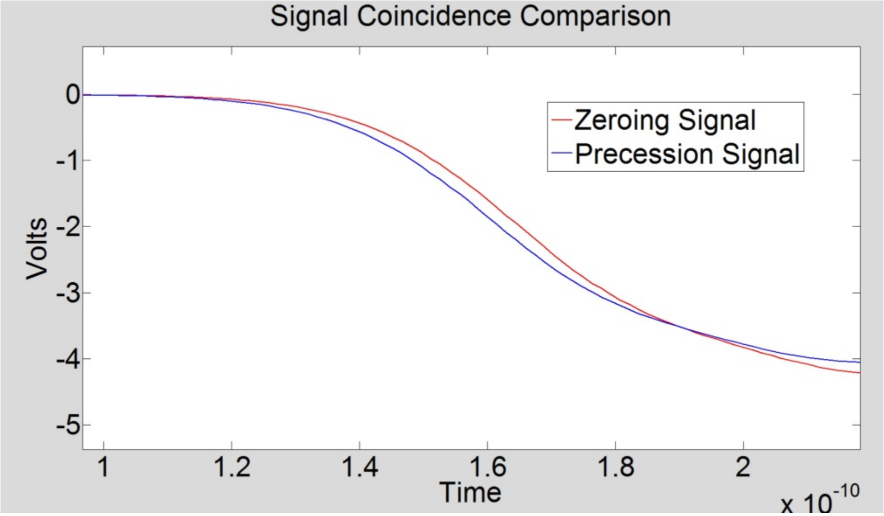

"Zeroing" step signal is not aligned in time with "Precession" step signal due to a *slight* drift in trigger signal.

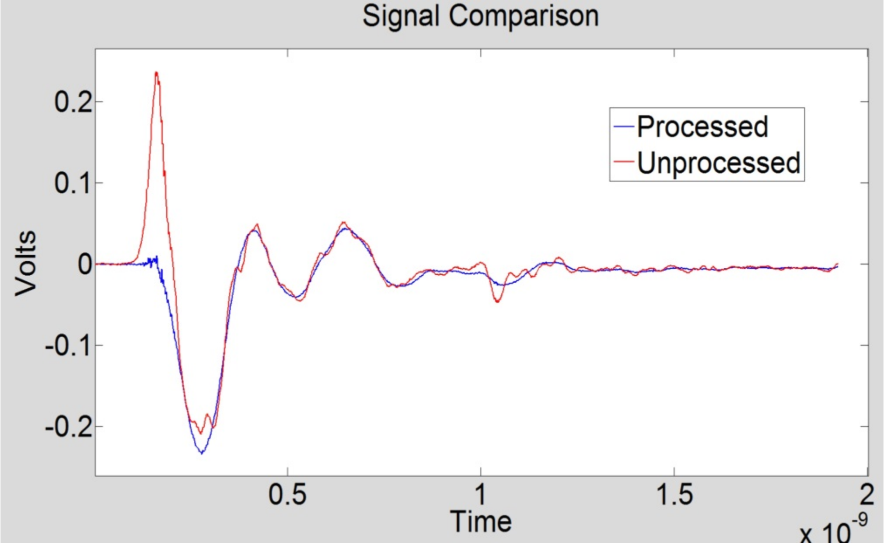

This introduces relatively large voltage spikes and an apparently noisy signal (red). Signals must be time shifted to correlate them between 0V and -2.5V. This yields the actual signal (blue).

UNIVERSITY OF SOUTH CAROLINA

Time-Domain Results

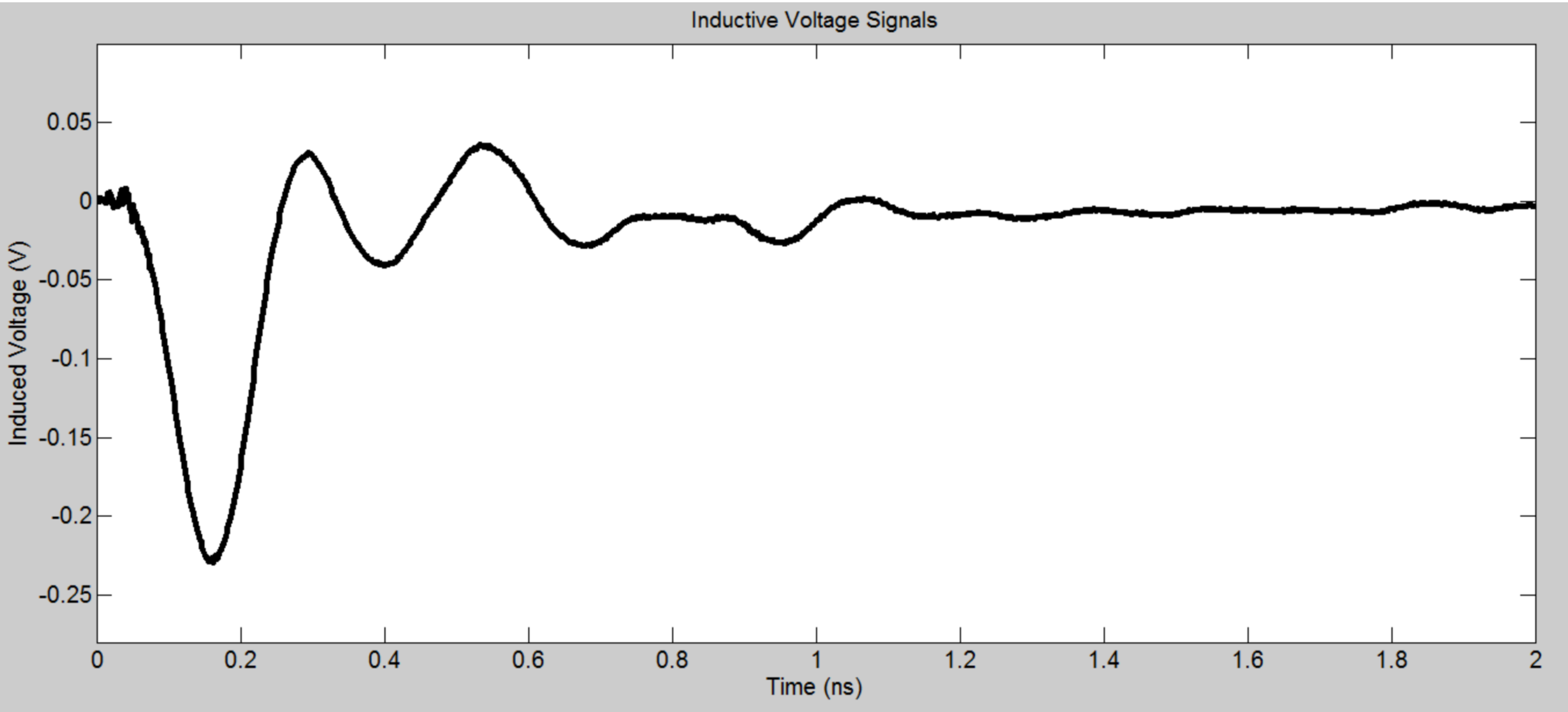

Example of a typical corrected measurement. Note the measured voltage signal is still not exactly a damped sine wave as predicted. Why?

UNIVERSITY OF SOUTH CAROLINA

FFT Results

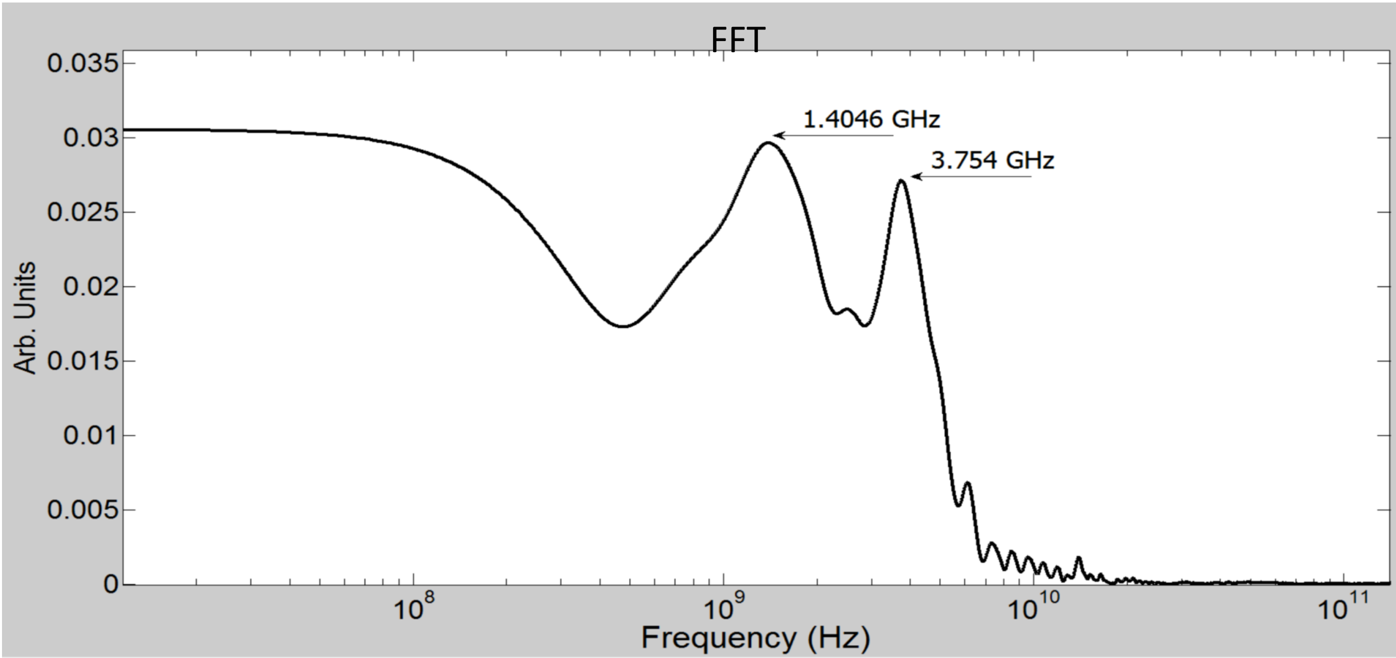

Two main resonance peaks are seen when an FFT is done on time-domain results. They must both be accounted for in a time domain data fit. The low frequency mode is the known resonant frequency of magnetite from FMR experiments. The definite origin of the higher mode is presently unknown.

UNIVERSITY OF SOUTH CAROLINA

Time-Domain Data Fit

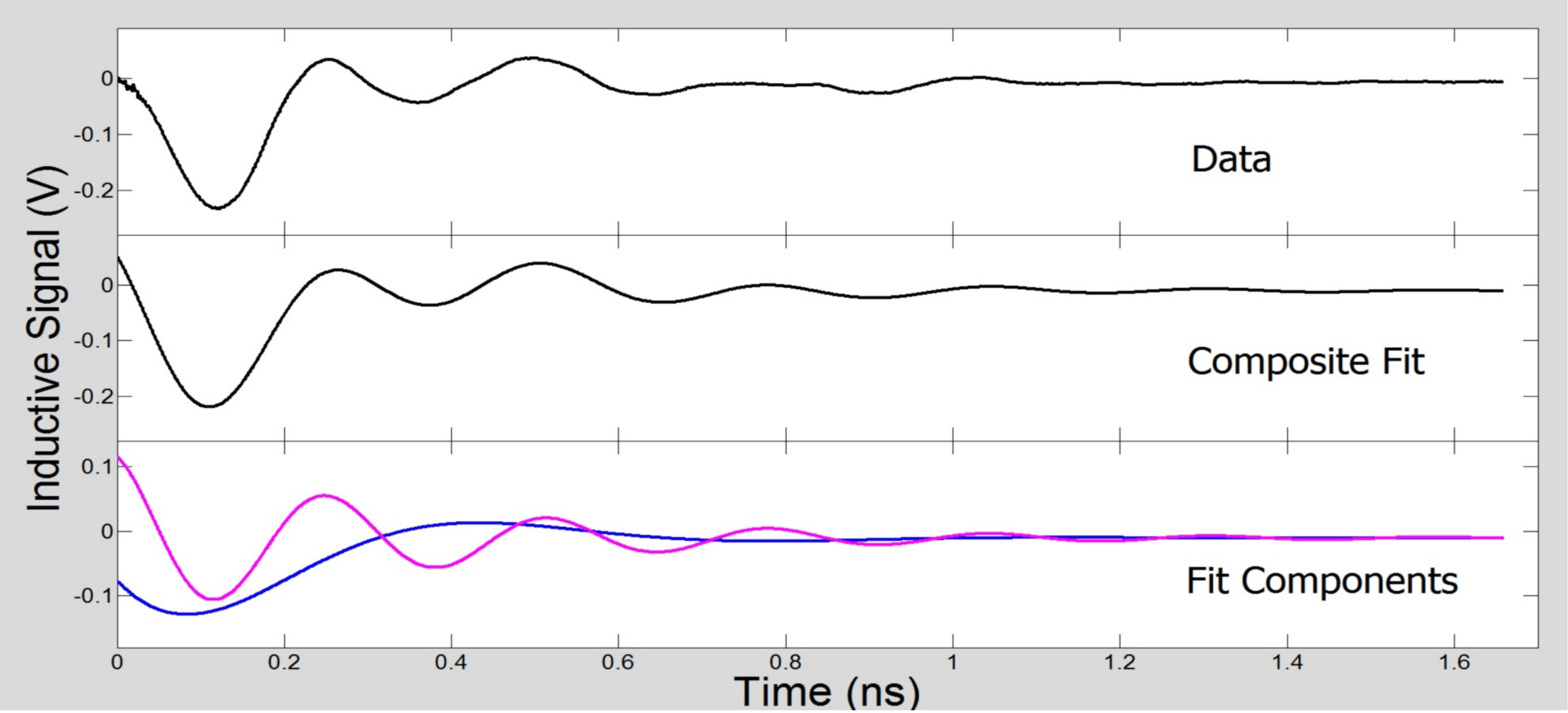

$$V(t) = V_1\, sin(\omega_{p1} t + \phi_1)\, e^{-t/\tau_1} + V_2\, sin(\omega_{p2} t + \phi_2)\, e^{-t/\tau_2}$$

UNIVERSITY OF SOUTH CAROLINA

Time-Domain Data Fit

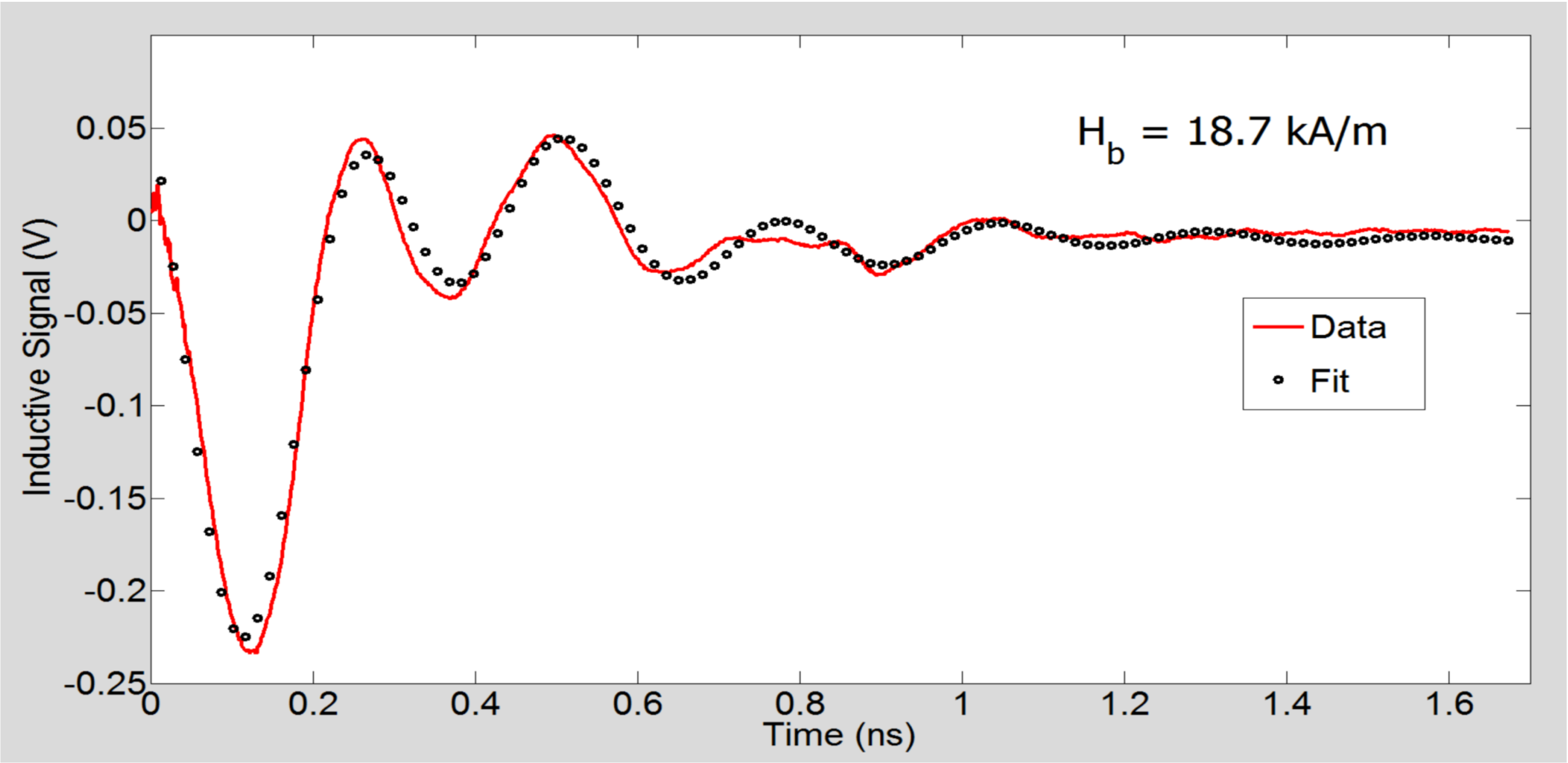

Circular field-dried data, results typical.

UNIVERSITY OF SOUTH CAROLINA

Time-Domain Data Fits

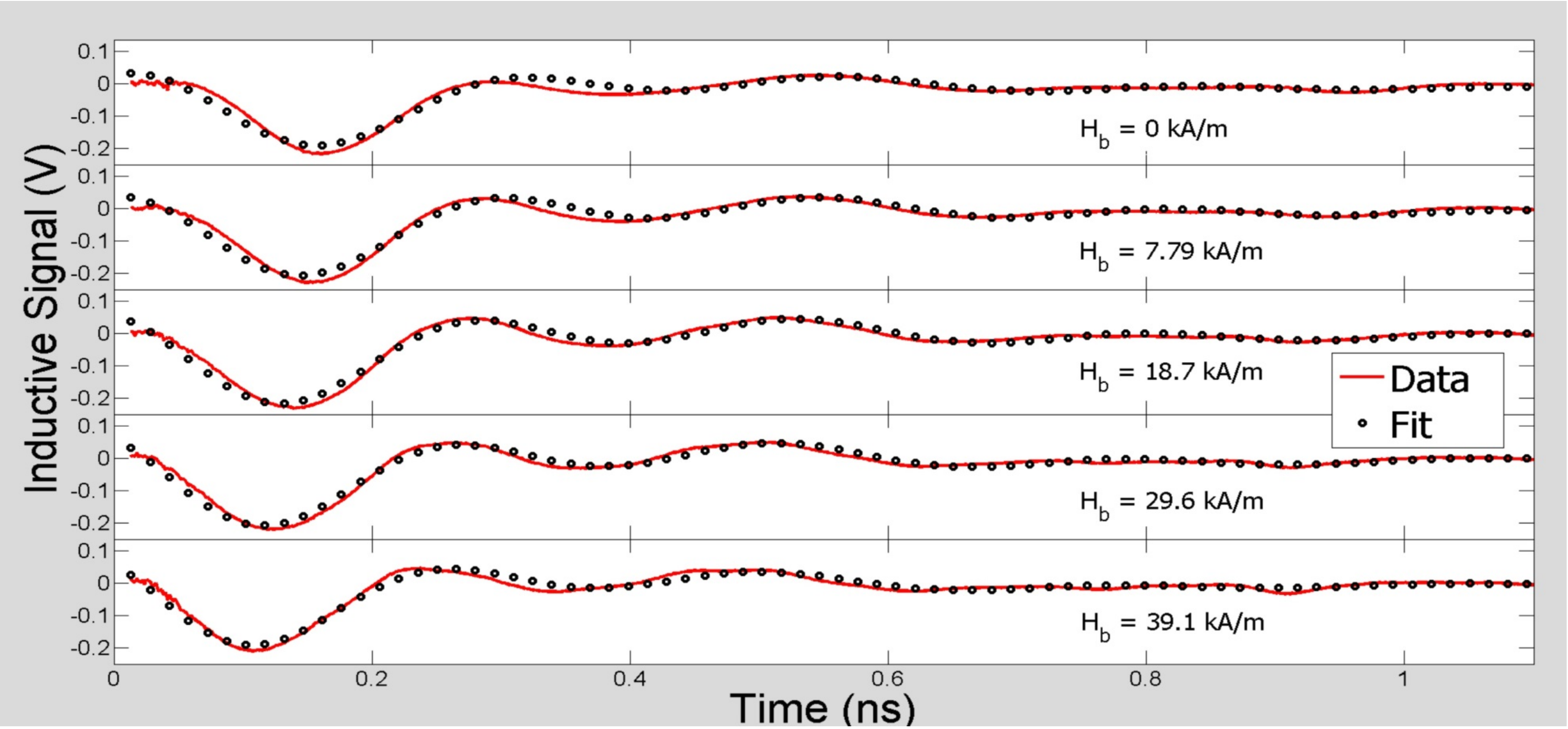

Circular field-dried data, results typical.

UNIVERSITY OF SOUTH CAROLINA

Low Frequency Mode

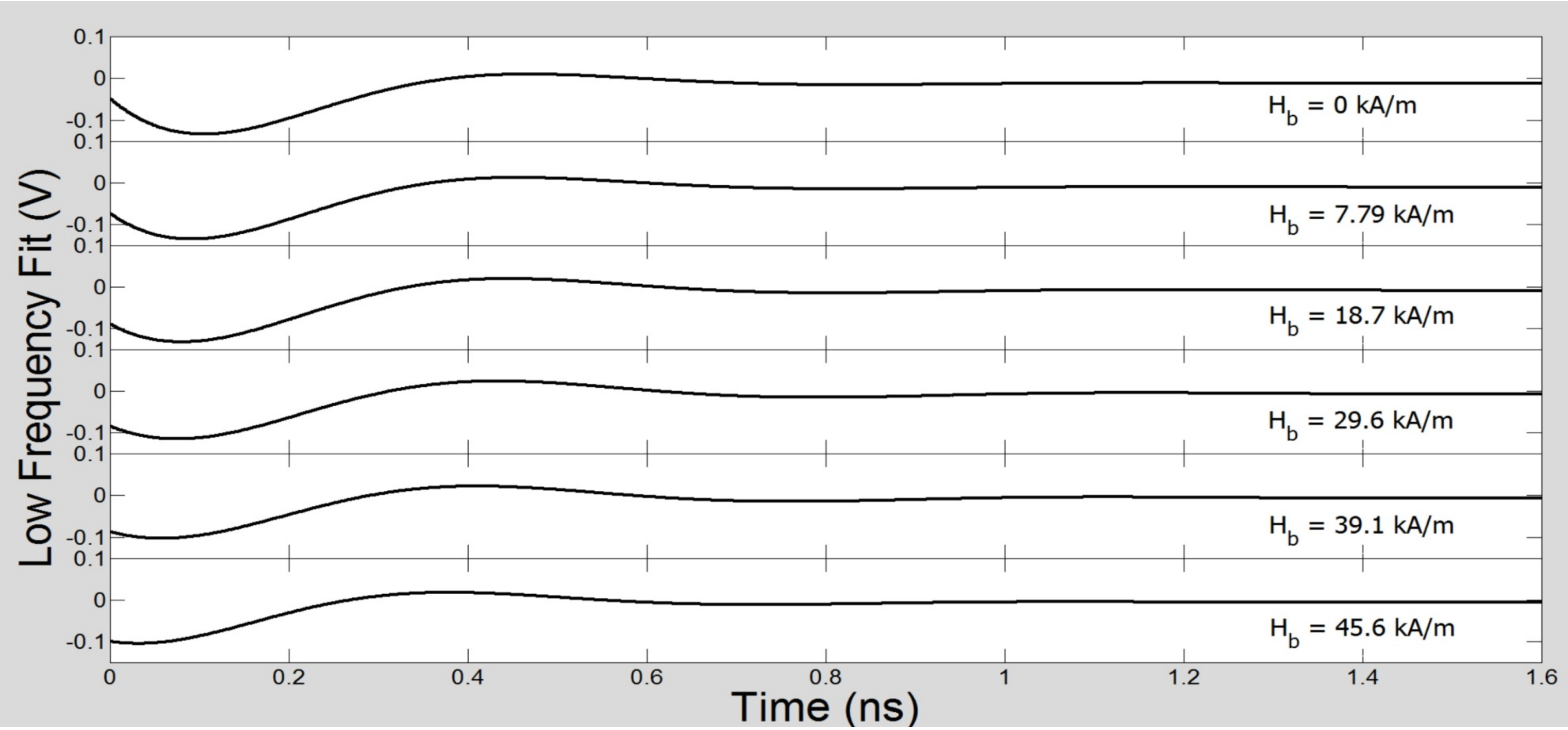

Circular field-dried data, results typical.

UNIVERSITY OF SOUTH CAROLINA

High Frequency Mode

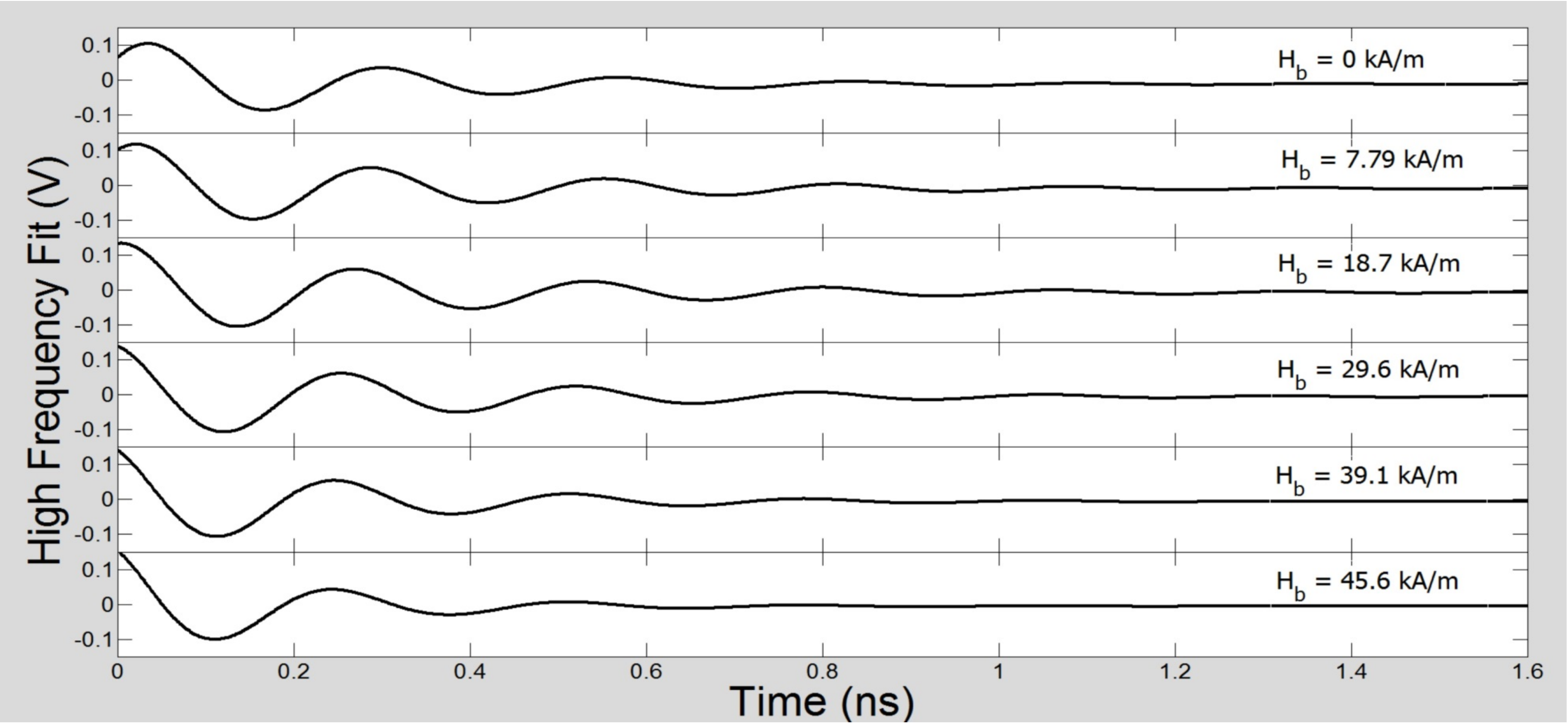

Circular field-dried data, results typical.

UNIVERSITY OF SOUTH CAROLINA

Frequency Domain Analysis

- The general Kittle equation of ferromagnetic resonance was modified to allow for the magnetization to be a function of the bias field (superparamagnetism).

$$f_p = g\frac{\mu_0\mu_B}{h}\sqrt{[(KH_b + H_A) + (\mathcal{N}_x - \mathcal{N}_z)M(H)]\left[(KH_b + H_A) + \left(\mathcal{N}_y - \mathcal{N}_z\right)M(H)\right]}$$

- H_A is determined from the frequency at $H_b = 0$.
- The bias field requires scaling to account for sample-wide demagnetization.
- The value of g is found by fitting the FFT results to this equation.
- The demagnetizing factors $\mathcal{N}_i$ determine the shape of the body that is resonating.
- Film (flat plane): $\mathcal{N}_x = 1$, $\mathcal{N}_y = \mathcal{N}_z = 0$. Then: $f_0 = \mu_0\gamma\sqrt{\left[H_0' + M(H)\right]H_0'}$
- Sphere: $\mathcal{N}_x = \mathcal{N}_y = \mathcal{N}_z = 1/3$. Then: $f_0 = \mu_0\gamma H_0'$
- It was unknown what a film composed of individual interacting spheres would do.

UNIVERSITY OF SOUTH CAROLINA

Frequency Domain Fit

Circular Field-Dried Data

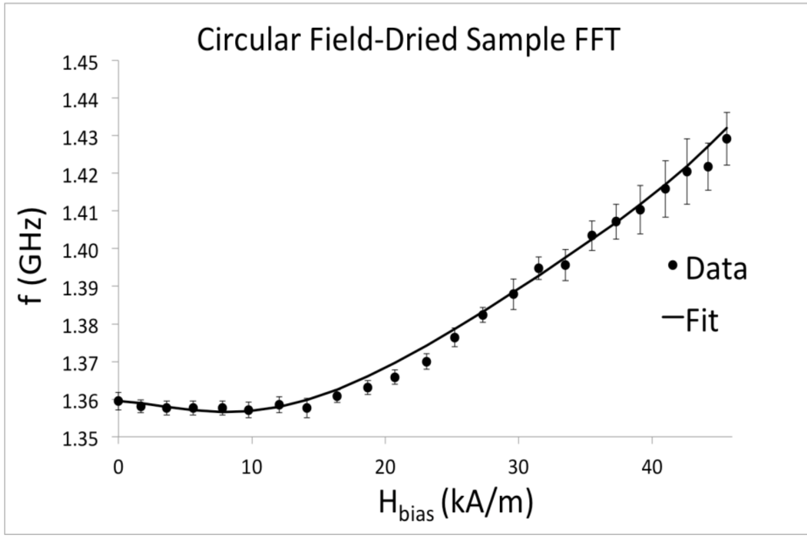

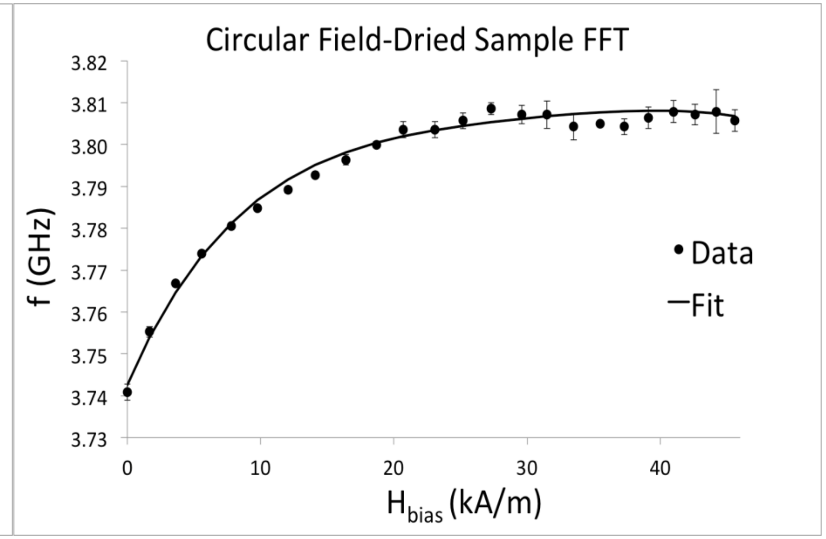

- $\mathcal{N}_x$=0.355$\pm$0.003, $\mathcal{N}_y$=0.309$\pm$0.003, and $\mathcal{N}_z$=0.335.
- Demagnetizing factors indicate nearly spherical behavior, not a collective behavior (e.g. film), but still *slightly* dependent on M(H), which is *nonlinear*.
- *g*=2.10$\pm$0.003. Within 1% error of a commonly cited value for single crystal magnetite particles (*g*=2.1). K=0.097$\pm$0.013 and H_A=38.5kA/m

UNIVERSITY OF SOUTH CAROLINA

Frequency Domain Fit

Strip Field-Dried Data

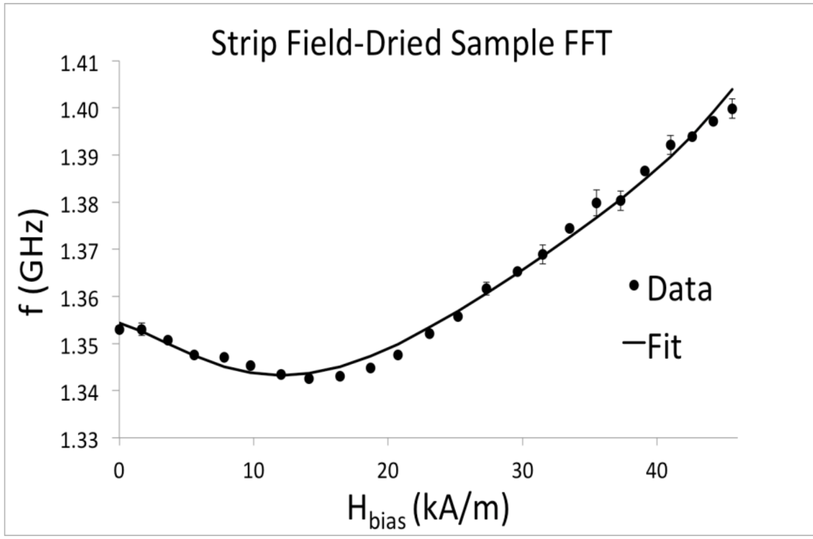

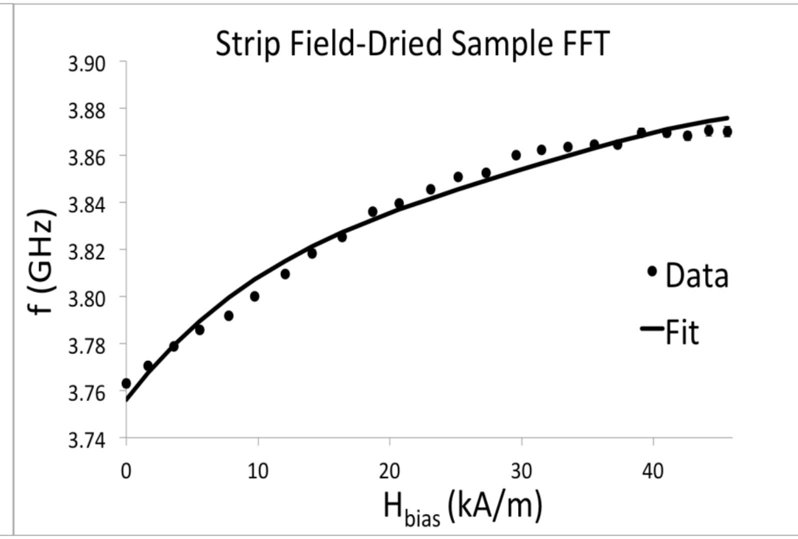

- $\mathcal{N}_x$=0.358±0.001, $\mathcal{N}_y$=0.306±0.001, and $\mathcal{N}_z$=0.335.
- Demagnetizing factors indicate nearly spherical behavior, not a collective behavior (e.g. film), but still *slightly* dependent on M(H), which is *nonlinear*.
- g=2.095±0.004. Less than 1% of the previously reported value for single crystal magnetite particles. K=0.095±0.002 and H_A=38.42kA/m

UNIVERSITY OF SOUTH CAROLINA

Frequency Domain Fit

Circular Non Field-Dried Data

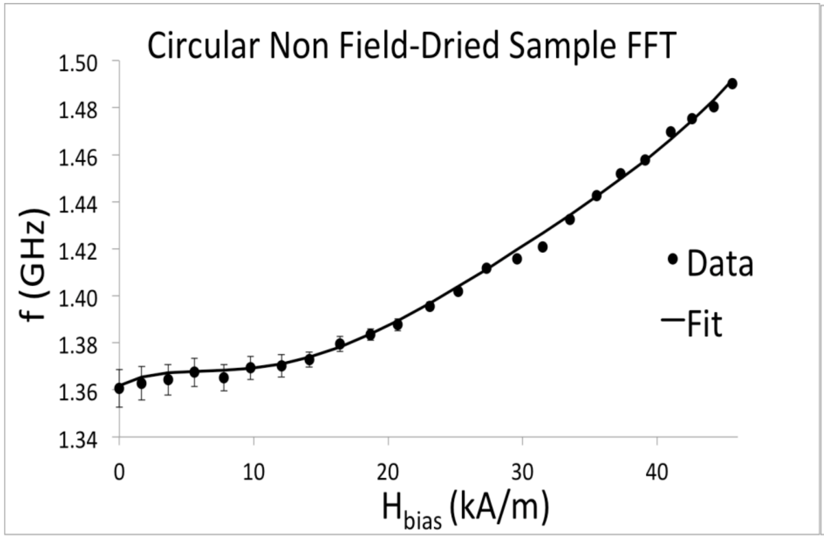

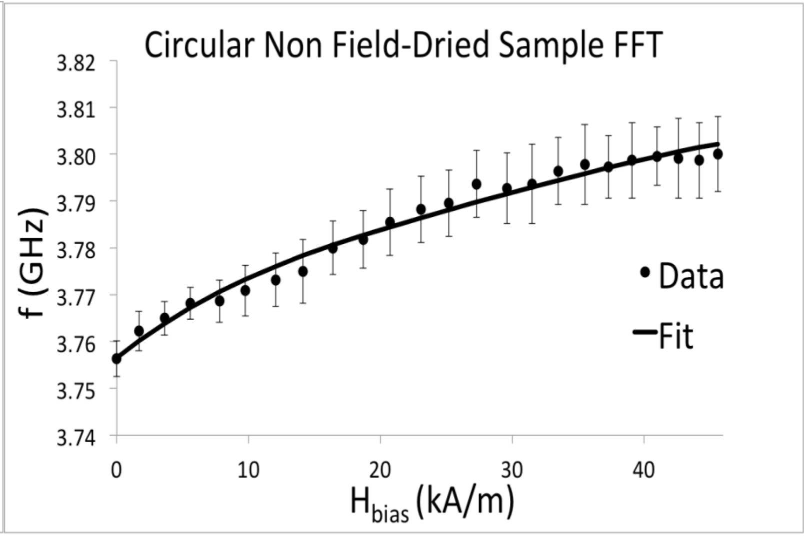

- $\mathcal{N}_x$=0.367$\pm$0.001, $\mathcal{N}_y$=0.298$\pm$0.001, and $\mathcal{N}_z$=0.3338.
- Demagnetizing factors indicate nearly spherical behavior, not a collective behavior (e.g. film), but still *slightly* dependent on M(H), which is *nonlinear*.
- g=2.24$\pm$0.014, which is approximately 7% error. K=0.1474$\pm$0.0008 and H_A=38.2kA/m.

UNIVERSITY OF SOUTH CAROLINA

Frequency Domain Fit

Strip Non Field-Dried Data

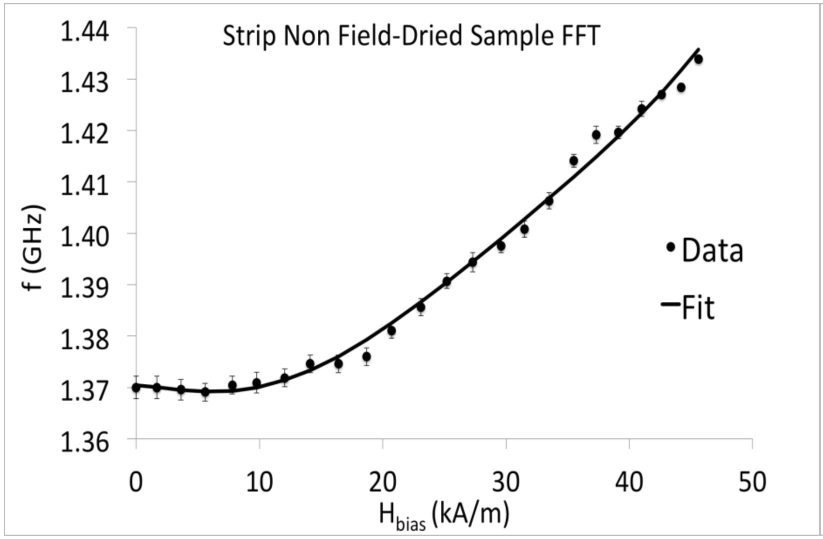

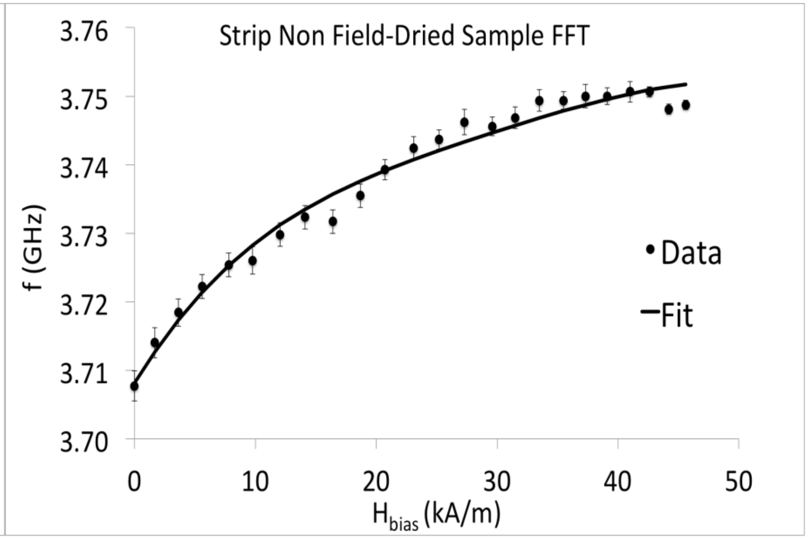

- $\mathcal{N}_x$=0.351$\pm$0.001, $\mathcal{N}_y$=0.313$\pm$0.001, and $\mathcal{N}_z$=0.335.
- Demagnetizing factors indicate nearly spherical behavior, not a collective behavior (e.g. film), but still *slightly* dependent on M(H), which is *nonlinear*.
- be *g*=2.118$\pm$0.004, which is within 1% error of previously reported value for single crystal magnetite particles. K=0.079$\pm$0.004 and H_A=38.8kA/m.

Frequency Domain Discussion

- The data are well fitted to the Kittle equation of ferromagnetic resonance where the demagnetizing factors are seen to describe spheres, not the overall sample.
- The scale factor K is found to be proportional to the H field, not the magnetization $M(H)$ as was expected for a demagnetization field. This is not presently understood.
- The quantity H_A may be attributed *to* the slight remanent field found earlier or possibly to the magnetocrystalline anisotropy field given by

$$H_A = \frac{2K_1}{\mu_0 M_s}$$

- Putting the values K_1 = 13kJ/m^3 and M_s = 480kA/m yields H_A = 43kA/m, which is within 10% of all values of H_A found from precession data at H_b = 0.
- If the largest value of M_s = 532kA/m found from the VSM is used, the error is less than 1%, however this measurement has 2 potential volumetric errors mentioned earlier.

UNIVERSITY OF SOUTH CAROLINA

Field-Dried Damping

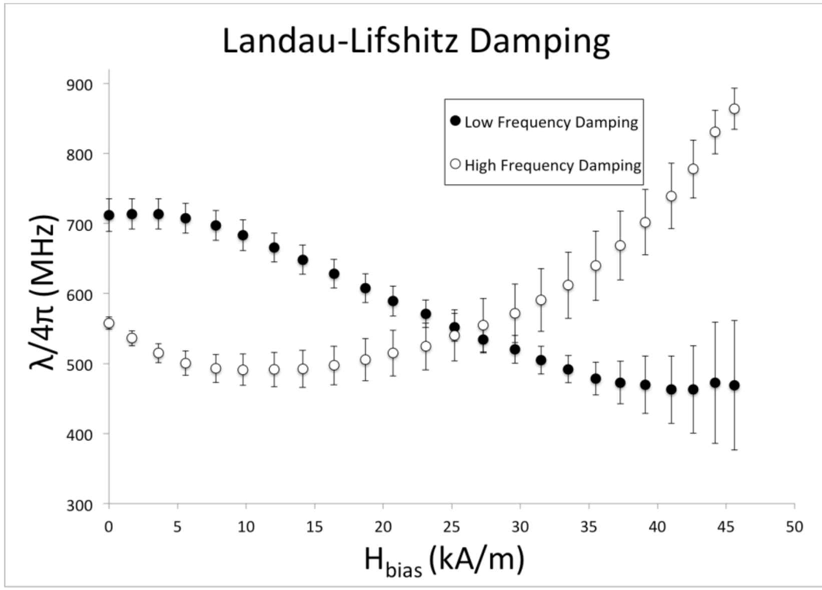

Circular field-dried damping.

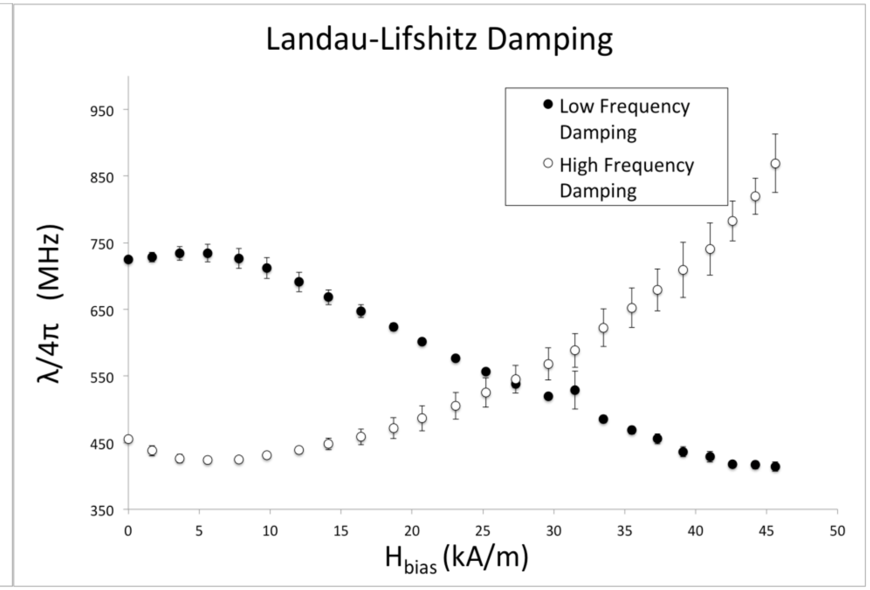

Strip field-dried damping.

- The low mode damping has a nearly monotonic decrease as bias field increases.
- The high mode reaches a minimum at different points and increases dramatically.

UNIVERSITY OF SOUTH CAROLINA

Non Field-Dried Damping

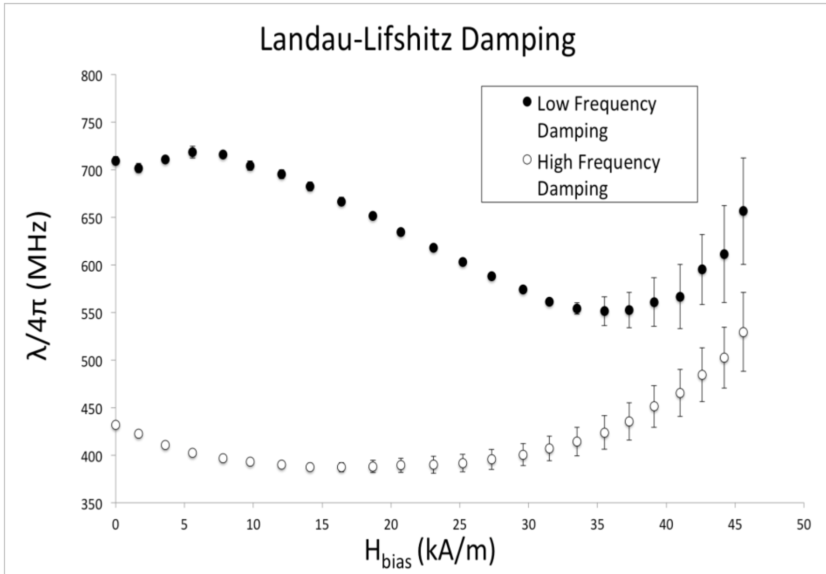

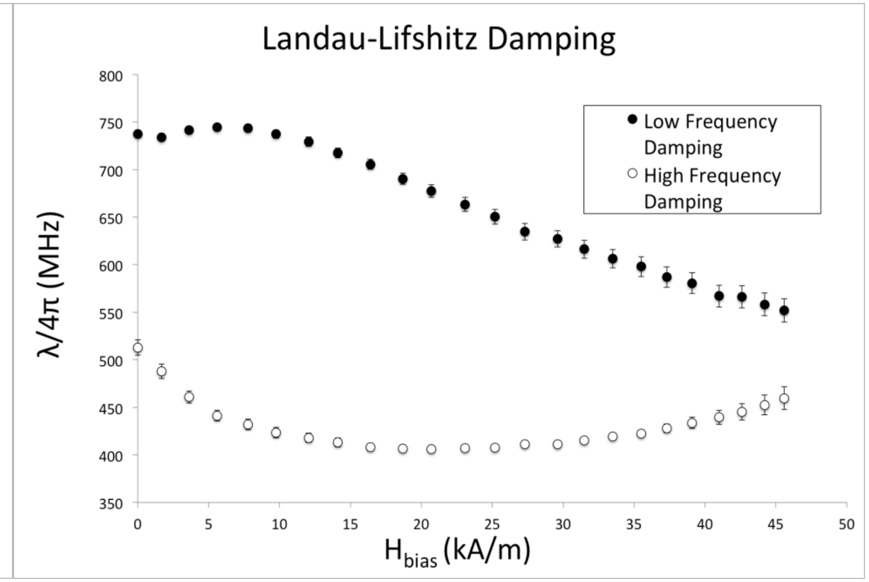

Circular non field-dried damping.

Strip non field-dried damping.

- The low mode damping for the strip has a nearly monotonic decrease as bias field increases but the circle increases (as does the error).
- The high mode reaches a minimum at different points and increases much less than for the field-dried case.

UNIVERSITY OF SOUTH CAROLINA

Conclusions

- The time-domain signals are well fitted to two exponentially damped sinusoids.
- The low frequency is the resonant frequency of magnetite, the origin of the higher mode has not been definitively identified.
- The samples all display behavior of nearly spherical objects for both frequencies.
- Field drying versus non field-drying the samples has little effect on the precession frequencies as does sample shape.
- The *g*-factors were found to agree well with the previously reported value.
- The bias field reduction was not found to be a function of the magnetization.
- Low frequency damping generally decreases with increasing bias field, a result similar (qualitatively) to impulse induction experiments on thin films.
- High frequency damping is largely affected by field drying. It increases dramatically at high bias fields.
- Due to damping almost all of the dynamics have dissipated within 2ns.

References

1) R. R. Shah, T. P. Davis, A. L. Glover, D. E. Nikkles, and C. S. Brazel, *J. Magn. Magn. Mater.* **387**, 96 (2015).
2) M. Swierczewska, S. Lee, X. Y. Chen, *Mol. Imaging* **10**, 3.
3) B. Gleich, J. Weizenecker, *Nature* **435**, 1214 (2005).
4) J. Kim, J. E. Lee, S. H. Lee, J. H. Yu, J. H. Lee, T. G. Park, T. Heyon, *Adv. Mater.* **20**, 478 (2008).
5) B. G. Krug and J. A. Asumadu, *IEEE*, **15**, 4174 (2015).
6) G.V. Kurlyandskaya, J. Cunanan, S.M. Bhagat, J.C. Aphesteguy, S.E. Jacobo, *J. Phys. Chem. Solids* **68**, 1527 (2007).
7) De Biasi , E. Lima Jr., C.A. Ramos, A. Butera, R.D. Zysler, *J. Magn. Magn. Mater.* **326**, 138 (2013).
8) Benjamin P. Weiss *et al*. *Earth. Planet. Sci. Lett*. **224**, 73 (2004).
9) Tamaru, J. A. Bain, R. J. M. van de Veerdonk, T. M. Crawford, M. Covington, and M. H. Kryder, *J. Appl. Phys*., **91**, 8034 (2002).

UNIVERSITY OF SOUTH CAROLINA

References

10) S. Kopyl *et al. J. Magn. Magn. Mater.* **358**, 44 (2014).
11) F. J Owens, *J. Phys. Chem. Solids* **64**, 2289 (2003).
12) M. Grimsditch, G. K. Leaf, H. G. Kaper, D. A. Karpeev, R. E. Camley, *Phys. Rev. B*. **69**, 174428 (2003).
13) J. M. D. Coey, *Magnetism and Magnetic Materials*, Cambridge Press, Cambridge (2010), p. 316.
14) T.J. Silva, C.S. Lee, T.M. Crawford, and C.T. Rogers, *J. Appl. Phys*. **85**, 7849 (1999).
15) L. Néel, *Ann. Geophys.* (*C. N. R. S.)* **5**, 99 (1949).
16) M. F. Hansen, P. E. Jonsson, P. Nordblad, P. Svedlindh, *J. Phys.:Condens. Matter* **14**, 4901 (2002).
17) D. Kechrakos, and K. N. Trohidou, *J. Nanosci. Nanotechnol.* **8**, 2929 (2008).
18) J. Lee, R. Tan, J. Wu, and Y. Kim, *Appl. Phys. Lett.* **99**, 062506 (2011).
19) X. Batlle and A Labarta, *J. Appl. Phys*. **35** R15-R42 (2002).

UNIVERSITY OF SOUTH CAROLINA

References

20) N. Song *et al.* *Sci. Rep*. **3**, 3161 (2013).
21) C. Kittel, *Phys. Rev*. **73**, 155–161 (1948).

UNIVERSITY OF SOUTH CAROLINA

Questions?

UNIVERSITY OF SOUTH CAROLINA